

178013: quartz diorite gneiss, Quartz Hill

Location and sampling

NULLAGINE (SF 51-5), NULLAGINE (2954)
MGA Zone 51, 214200E 7566640N

Sampled on 27 May 2002

The sample was taken from a 2 m-high rock on the northeastern edge of a 40 × 15 m, low rocky pavement, 150 m east of the access track and 2.3 km south-southwest of Quartz Hill.

Tectonic unit/relations

The sample is a pale-grey, medium- and even-grained, foliated quartz diorite gneiss from the Golden Eagle Orthogneiss in the Kurrana Granitoid Complex, Kurrana Terrane (Bagas, 2005). The sample collected contains at least two igneous phases — a coarse-grained pegmatite and an equigranular quartz diorite — and was collected to constrain the crystallization age of the quartz diorite precursor to the gneiss. The Golden Eagle orthogneiss has previously been dated at 3178–3150 Ma by Nelson (2004a; GSWA 178012).

Petrographic description

The principal minerals in the sample are plagioclase (75–80 vol.%), quartz (15 vol.%), microcline (5 vol.%), and biotite (2–3 vol.%), with trace amounts of accessory titanite, apatite, allanite, opaque oxide, and zircon. This is a weakly altered, medium- to fine-grained, quartz diorite gneiss with sericite–clinozoisite–chlorite–epidote–carbonate alteration and a band of altered monzogranite gneiss, similarly altered but with stilpnomelane and no carbonate. The diorite probably underwent high-grade metamorphism followed by low-temperature hydrothermal alteration. The hand specimen has a foliation defined by parallel lenses of quartz, and is typically poor in K-feldspar but has a band rich in quartz and K-feldspar close to its margin. This band is about 10 mm wide, and comprises microcline (30–35 vol.%), quartz (30 vol.%), plagioclase (possibly andesine; 30 vol.%), and biotite (7 vol.%), with accessory titanite (trace), opaque oxide (trace), and apatite (trace), indicating it is a monzogranite. In the host-rock, there are scattered anhedral augen of plagioclase, up to 6 mm long, with irregular areas dusted by sericite and clinozoisite. In some grains, the alteration is intense, with minor granular epidote and decussate muscovite, passing into definite saussuritic alteration. Medium-sized plagioclase grains, mostly 1 to 2 mm in length, are typically fresher than the larger grains, as are smaller recrystallized grains, typically 0.2 to 0.5 mm in diameter, in small lenses of micromosaic. Minor microcline is included in plagioclase, is a component in the micromosaic lenses (with minor myrmekite), and forms separate grains up to 1 mm long and locally intergrown with plagioclase. Rare examples of oriented rods of K-feldspar

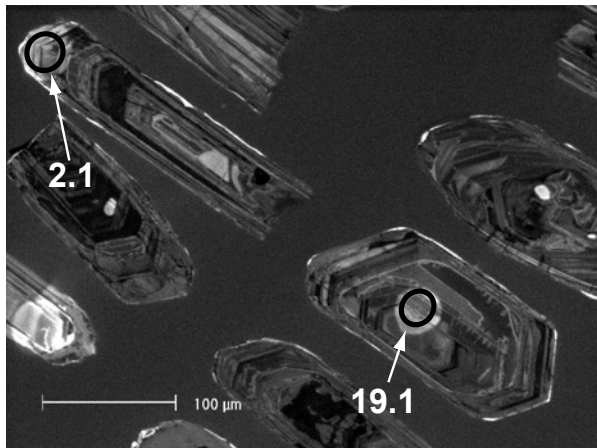
in plagioclase suggest an antiperthitic texture. A wavy foliation throughout the rock is defined by lenses of quartz up to 5 mm long, and largely composed of grains less than 2 mm in length. Biotite is present as flakes up to 0.5 mm long and oriented parallel to the foliation, disseminated, and in small lenses, but it is altered to chlorite and leucoxene, locally with minor to abundant epidote. There are also rare aggregates of carbonate, epidote, and chlorite of uncertain origin, possibly derived from amphibole rather than biotite. Some of the more biotite-rich lenses contain minor titanite, and there is rare opaque oxide, commonly mantled by epidote. Rare allanite occurs as small prisms, with fresh and altered zones, and mantled by epidote. Minor apatite is disseminated but zircon is rare and very fine grained ($\leq 40 \mu\text{m}$ in diameter). The monzogranite band has elliptical augen of microcline and plagioclase up to 5 mm long, as well as abundant recrystallized feldspars, mostly less than 0.8 mm in grain size, with weak alteration of the plagioclase as in the host-rock. Some of the larger plagioclase grains are probably antiperthitic. Quartz forms bands parallel to the foliation, as in the host-rock, but they are wider (up to 2 mm), and more continuous and abundant. There are also bands rich in schistose biotite, up to 1 mm in grain size, and now totally altered to chlorite–leucoxene(–clay), with minor granular epidote. Minor to abundant titanite is present in the biotite-rich bands, and there is accessory apatite as well as rare opaque oxide. Small aggregates of orangish-brown ferristilpnomelane are present, but zircon is apparently absent. The possibility of antiperthitic plagioclase suggests initially higher grade metamorphism (upper amphibolite to granulite facies), followed by low-temperature hydrothermal alteration. The rare stilpnomelane suggests some oxidation in the monzogranite band.

Zircon morphology

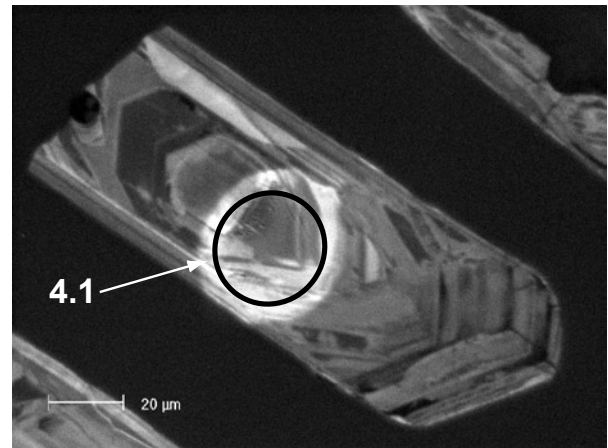
The zircons isolated from this sample are typically colourless, pale yellowish-brown or dark brown, between $60 \times 140 \mu\text{m}$ and $160 \times 280 \mu\text{m}$ in size, and elongate and euhedral or subhedral. Many grains have faint internal zonation, whereas a minority are structureless or have unzoned interiors surrounded by zoned rims, but contain abundant fluid and mineral inclusions. Cathodoluminescence images of representative zircons are given in Figure 1.

Analytical details

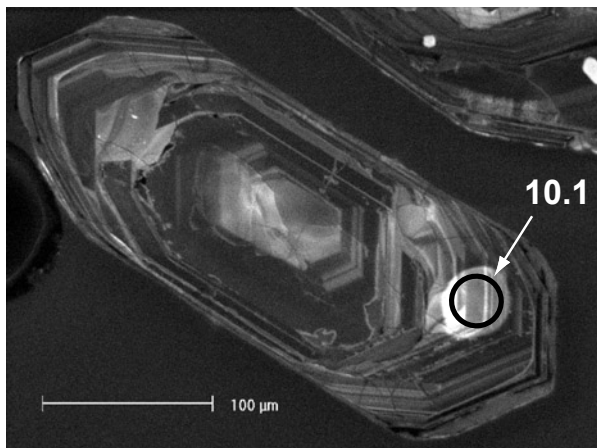
This sample was analysed on 10 and 26 February 2003. The counter deadtime during both analysis sessions was 24 ns. During the first analysis session, seven analyses of the CZ3 standard were obtained. Following deletion of one standard analysis as an outlier, the remaining six standard analyses indicated a Pb*/U calibration uncertainty of 2.46% (1σ). Analyses 1.1 to 12.1 were obtained during the first analysis session. During the second analysis session, six analyses of



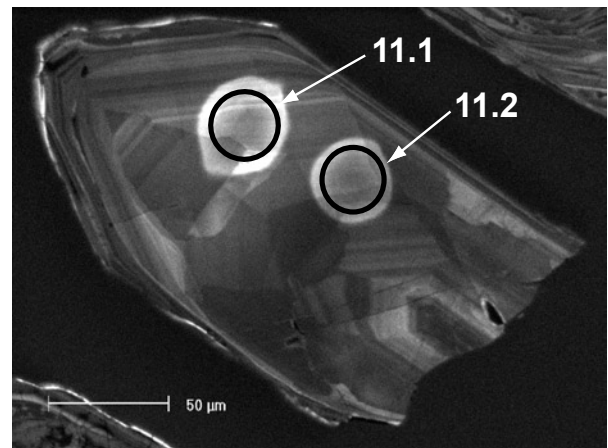
(a)



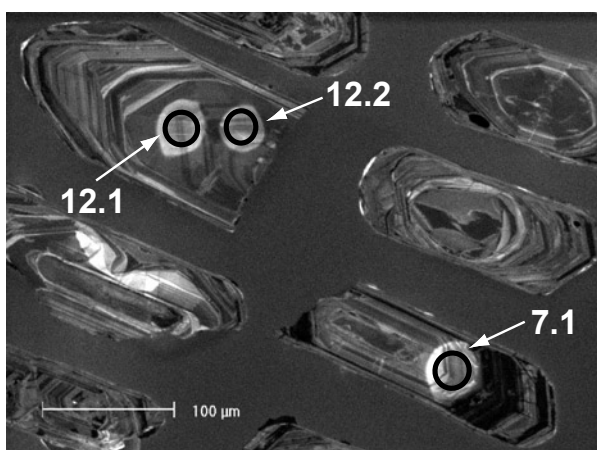
(b)



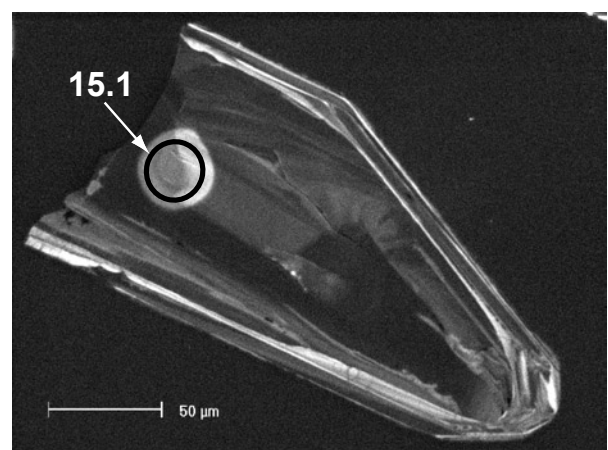
(c)



(d)



(e)



(f)

Figure 1. Cathodoluminescence images of representative zircons from sample 178013: quartz diorite gneiss, Quartz Hill

Table 1. Ion microprobe analytical results for zircons from sample 178013: quartz diorite gneiss, Quartz Hill

Grain spot	U (ppm)	Th (ppm)	Pb (ppm)	f206%	$^{207}\text{Pb}/^{206}\text{Pb}$	$\pm 1\sigma$	$^{208}\text{Pb}/^{206}\text{Pb}$	$\pm 1\sigma$	$^{206}\text{Pb}/^{238}\text{U}$	$\pm 1\sigma$	$^{207}\text{Pb}/^{235}\text{U}$	$\pm 1\sigma$	% concordance	Age	$\pm 1\sigma$
1.1	321	153	211	0.396	0.24822	0.00063	0.13939	0.00090	0.5424	0.0134	18.564	0.467	88	3 173	4
2.1	2021	1 243	517	0.322	0.15253	0.00030	0.14526	0.00051	0.2263	0.0056	4.759	0.119	55	2 374	3
3.1	548	203	319	0.055	0.24271	0.00045	0.11843	0.00047	0.4961	0.0122	16.602	0.415	83	3 138	3
4.1	602	372	449	0.331	0.25243	0.00044	0.17153	0.00061	0.6011	0.0148	20.921	0.522	95	3 200	3
5.1	269	178	203	0.182	0.25262	0.00061	0.17726	0.00082	0.6115	0.0151	21.298	0.536	96	3 201	4
6.1	420	264	296	0.380	0.24855	0.00052	0.17176	0.00076	0.5683	0.0140	19.474	0.488	91	3 176	3
7.1	259	68	185	0.757	0.25248	0.00074	0.07777	0.00112	0.6078	0.0150	21.158	0.535	96	3 200	5
8.1	869	594	462	0.143	0.25263	0.00038	0.17732	0.00048	0.4298	0.0106	14.971	0.373	72	3 201	2
9.1	316	744	141	0.828	0.24658	0.00088	0.11226	0.00142	0.3695	0.0091	12.561	0.319	64	3 163	6
10.1	308	137	223	0.153	0.25466	0.00056	0.09602	0.00062	0.6196	0.0153	21.756	0.546	97	3 214	3
11.1	155	82	119	0.052	0.25605	0.00078	0.13879	0.00085	0.6355	0.0158	22.437	0.569	98	3 223	5
12.1	293	108	216	0.026	0.25685	0.00055	0.09797	0.00048	0.6296	0.0156	22.296	0.559	98	3 227	3
13.1	157	54	113	0.364	0.25122	0.00090	0.09279	0.00130	0.6157	0.0065	21.326	0.247	97	3 192	6
14.1	269	85	197	0.103	0.25705	0.00062	0.08408	0.00069	0.6345	0.0066	22.487	0.245	98	3 229	4
15.1	401	53	312	0.147	0.28294	0.00051	0.03596	0.00048	0.6823	0.0070	26.619	0.282	99	3 379	3
16.1	105	38	77	0.101	0.25305	0.00099	0.09801	0.00115	0.6264	0.0068	21.856	0.263	98	3 204	6
11.2	216	134	171	0.083	0.25664	0.00067	0.16401	0.00082	0.6454	0.0067	22.837	0.253	99	3 226	4
12.2	307	116	232	0.091	0.25580	0.00057	0.10008	0.00063	0.6445	0.0066	22.732	0.246	100	3 221	4
17.1	281	57	192	0.195	0.25096	0.00063	0.04981	0.00070	0.6071	0.0063	21.007	0.230	96	3 191	4
18.1	362	161	272	0.093	0.25230	0.00052	0.12113	0.00060	0.6349	0.0065	22.086	0.236	99	3 199	3
19.1	519	138	297	0.395	0.23757	0.00053	0.06784	0.00074	0.5019	0.0051	16.439	0.176	84	3 104	4

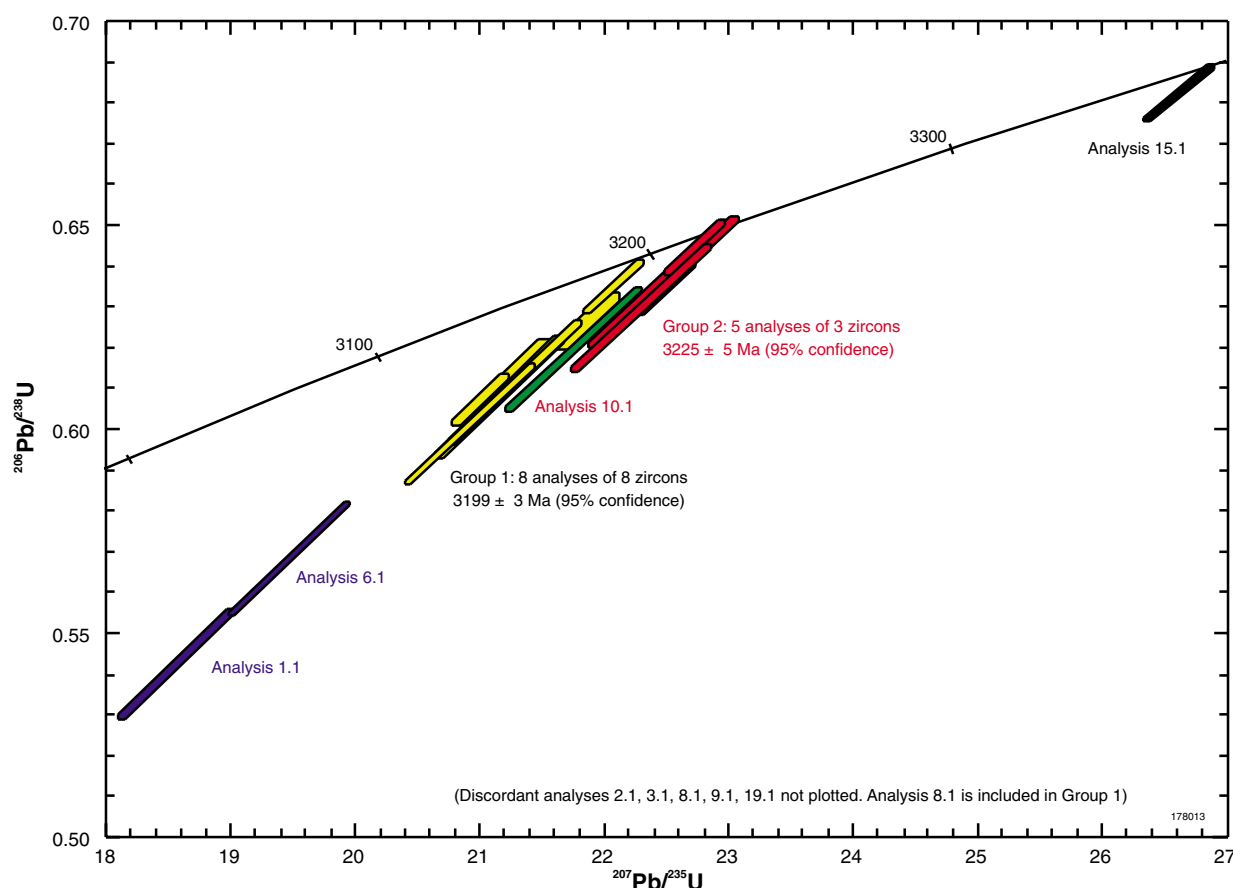


Figure 2. Concordia plot for sample 178013: quartz diorite gneiss, Quartz Hill

the CZ3 standard indicated a Pb^*/U calibration uncertainty of 0.685% (1σ). A calibration uncertainty of 1.0% (1σ) was applied to analyses of unknowns obtained during this analysis session. Common-Pb corrections were applied assuming Broken Hill common-Pb isotopic compositions for all analyses, with the exception of analyses 1.1, 2.1, 4.1, 6.1, 7.1, 8.1, 9.1, 10.1, and 19.1, for which isotopic compositions determined using the method of Cumming and Richards (1975) were assumed.

Results

Twenty-one analyses were obtained from 19 zircons. Results are given in Table 1 and shown on a concordia plot in Figure 2.

Interpretation

The analyses are concordant to highly discordant, with the discordance pattern consistent with a single ancient episode of radiogenic-Pb loss. On the basis of their $^{207}\text{Pb}/^{206}\text{Pb}$ ratios, many analyses can be assigned to one of two groups. Eight slightly discordant analyses of eight zircons (4.1, 5.1, 7.1, 8.1, 13.1, 16.1, 17.1, 18.1), assigned to Group 1, have $^{207}\text{Pb}/^{206}\text{Pb}$ ratios defining a single population and indicating a weighted mean $^{207}\text{Pb}/^{206}\text{Pb}$ date of 3199 ± 3 Ma (chi-squared = 0.99). Five concordant and slightly discordant analyses of

three zircons (11.1, 11.2, 12.1, 12.2, 14.1), assigned to Group 2, have $^{207}\text{Pb}/^{206}\text{Pb}$ ratios defining a single population and indicating a weighted mean $^{207}\text{Pb}/^{206}\text{Pb}$ date of 3225 ± 5 Ma (chi-squared = 0.64). Slightly discordant analysis 10.1 indicates a $^{207}\text{Pb}/^{206}\text{Pb}$ date that is intermediate between those of Groups 1 and 2, and highly discordant analyses 2.1, 3.1, 9.1, and 19.1 indicate younger $^{207}\text{Pb}/^{206}\text{Pb}$ dates, whereas concordant analysis 15.1 indicates a substantially older $^{207}\text{Pb}/^{206}\text{Pb}$ date than those of Group 2.

The date of 3225 ± 5 Ma indicated by the weighted mean $^{207}\text{Pb}/^{206}\text{Pb}$ ratio of the five concordant and slightly discordant analyses of three zircons of Group 2 is interpreted as the age of igneous crystallization of the dioritic precursor to the gneiss. The older $^{207}\text{Pb}/^{206}\text{Pb}$ date indicated by concordant analysis 15.1 is interpreted to be of a xenocryst zircon. The slightly younger $^{207}\text{Pb}/^{206}\text{Pb}$ dates indicated by the slightly discordant analyses of Group 1, and the remaining highly discordant analyses, are interpreted to be of analysis sites that have lost radiogenic Pb during an ancient disturbance event.

Recommended reference for this publication:

NELSON, D. R., 2005, 178013: quartz diorite gneiss, Quartz Hill; Geochronology dataset 550; in Compilation of geochronology data, June 2006 update: Western Australia Geological Survey.

Data obtained: 26/02/2003; Data released: 30/06/2005